Iron based 1D Nanostructures by Electrospinning Process

Cynthia Eid*,**, Arnaud Brioude*, Vincent Salles*, Jean-Claude Plenet****, Roy Asmar**, Yves Monteil*, Randa Khoury***, Antonio Khoury**, Philippe Miele*

*Laboratoire des Multimatériaux et Interfaces (UMR CNRS 5615), Université Lyon1, Université de Lyon, 43 Bd du 11 Novembre 1918, Villeurbanne Cedex, France.
**Laboratoire de Physique Appliquée (LPA) associé à l'école doctorale des Sciences et Technologies, Département de Physique, Université Libanaise, Faculté des Sciences II, 90656 Jdeidet El Metn, Liban.
***Laboratoire de Chimie, Faculté d'Agronomie, Université Libanaise, Fanar, Faculté des Sciences II, 90656 Jdeidet El Metn, Liban.
****Laboratoire de Physique de la Matière condensée et Nanostructures, CNRS UMR 5586, Université Lyon1, Université de Lyon, 43 Bd du 11 Novembre 1918, Villeurbanne Cedex, France.

ABSTRACT

We have successfully prepared iron based 1D nanostructures by electrospinning technique, varying the pyrolysis atmosphere. We have obtained hematite nanotubes and polycrystalline Fe_3C nanofibers by a simple air or mixed (H_2, Ar) annealing treatments respectively. In the first case, the direct influence of the starting polymer solution on the tubular morphology is of main importance and allows varying the wall thickness. In the second case, for the first time, we achieve to obtain polycrystalline Fe_3C nanofibers composed of carbon graphitic planes ensuring the Fe_3C nanoparticles stability and the nanofibers cohesion. The morphology and the structural properties have been studied by SEM, TEM, XRD and Raman spectroscopy.

Keywords: 1D nanomaterials, electrospinning, iron carbide, hematite, nanotubes

1 INTRODUCTION

Due to their strong shape anisotropy, one-dimensional (1D) nanomaterials, including nanotubes, nanowires and nanofibers exhibit specific properties that are not observed in the case of their bulk or particle counterparts [1]. Particularly, magnetic nanostructures have a considerable interest for many applications such as high-density magnetic recording, spintronics devices as well as the fabrication of sensors [2, 3].This can be explained by the geometrical dimensions of those nanostructures that are comparable with magnetic length scales such as exchange length and domain wall width [4]. Moreover, when such nanomaterials display a superparamagnetic behavior, they are of interest for a broad range of applications in drug delivery, for clinical diagnostic and therapeutic applications [5]. For example, the tubular structure of magnetic nanotubes presents an important advantage as its distinctive inner and outer surfaces can be differently functionalized [6].

More recently, the research of synthetic methods for ferric nanomaterials production has attracted considerable attention. Hematite (α-Fe_2O_3), the most stable iron oxide under ambient conditions, is commonly used in catalysts [7], gas-sensing materials [8] and pigments [9]. Magnetite (Fe_3O_4) is by far the most studied phase and is applied for biomedical applications being environmental friendly, easy to synthesize and presenting a high saturation magnetization [10]. Maghemite (γ-Fe_2O_3) which is one of the mostly used iron oxide for the industrial applications is of great importance in magnetic recording materials [11]. Up to nowadays, various methods have been used for the synthesis of 1D iron oxide nanomaterials such as hydrogen reduction in nanochannels [12], template directed growth [13,6], Hydrothermal/solvothermal processes [14-16]. In those methods, the aspect ratio is sometimes limited, and the amount of materials that can be produced is often restricted. Template methods usually encounter difficulties with the pre-fabrication and removal steps. Moreover, the final materials contain some impurities and strong aggregation effects can take place when anisotropic materials are involved, affecting the magnetization behavior considerably [17,18]. As a consequence, the preparation of ultrathin 1D-nanomaterials by a simple and versatile method is challenging.

Here, we have chosen the promising alternative of the electrospinning process that is an effective way to produce nanofibers with tunable properties [19]. Besides, it offers the possibility to easily generate macroscopic amounts of 1D-nanostructures from several materials [20]. Fe-based 1D-nanomaterials are obtained by electrospinning of a polymer solution of iron acetate. We would like to point out that the annealing treatments using air and hydrogen allow us to obtain hematite nanotubes and Fe_3C nanowires respectively. A study on the morphology and the structure of the produced materials is presented. The concentration of the polymer solution is varied as well, showing its direct

effect on the diameter of the as-prepared nanotubes and nanowires.

2 EXPERIMENTS

In a typical synthesis, 7 wt% PVP (polyvinyl pyrrolydone, Mw ~ 1.300.000, Acros Organics) solution with absolute ethanol (EtOH) as solvent was first prepared. 1 ml of acetic acid and 7 ml of the polymer solution were added into 1 g of iron acetate (Aldrich) as already detailed by E Santala *et al* [22] for the synthesis of Fe_2O_3 fibers combining electrospinning and atomic layer deposition (ALD) techniques. The solution was then mixed for 4 h before its use. In a typical electrospinning process, the polymer solution is extruded through a nozzle to which a high voltage is applied. The electrostatic forces, overcoming the surface tension of the solution, cause the ejection of a thin jet (from the needle tip) which is accelerated toward the grounded target [8, 20]. The resulting nanofibers are collected as an interconnected network of thin filaments on the surface of a metallic target [21].

In our experiment, the electrospinning was made by applying a high voltage (15 kV) to a droplet of the polymer solution at the apex of a sharp conducting needle. This jet speeded up by the electric field was collected on a static metallic substrate directly connected to the ground. Using a syringe-pump, the precursor solution placed into a plastic syringe was delivered to the metal needle at a constant flow rate of 0.6 ml h^{-1}. The working distance between the needle and the substrate was set to 15 cm.

$FeAc_2$/PVP Ratio	Before Annealing	Pyrolysis in air	Pyrolysis in H_2
2.63	A1	B1	C1
1.75	A2	B2	C2
0.87	A3	B3	C3
0.43	A4	B4	C4

Table 1. Samples prepared for different Iron acetate/PVP ratios. Samples denoted A, B and C are respectively not annealed, annealed under air and under H_2 flow.

The as-collected nanofibers PVP/$FeAc_2$ were then annealed following two methods: (i) in air in a tubular furnace at a heating rate of 5°C min^{-1} from room temperature to 550°C. (ii) As-collected nanofibers PVP/$FeAc_2$ were reduced at 350°C for 4 h under a hydrogenated atmosphere (5% H_2, 95 % Ar) at a heating rate of 3°C $min^{-1}$and cooled to room temperature over a period of 12 hours. The table 1 summarizes the samples realized by those two annealing treatment.

The morphology of the samples was analyzed by Scanning Electron Microscopy SEM (Hitachi S800) and their structural properties were studied by Transmission Electron Microscopy (TEM) in high resolution mode with a TOPCON 002B working at 200 kV. Raman spectra have been obtained from a Renishaw model RM 1000 Raman microscope operating at wavelength λ = 514.5 nm. The X-ray diffraction (XRD) pattern of products was recorded by step scan in the Philips (Almelo, Netherlands) X-ray diffractometer with Cu Kα radiation (l = 0.15406 nm) at 40 kV and 30 mA.

3 RESULTS AND DISCUSSIONS

We have first studied the crude samples (Samples A in table 1) obtained after the electrospinning process and before the annealing treatment., The Figure 1a shows the SEM images of PVP/$FeAc_2$ nanofibers prepared with the ratio of $FeAc_2$/PVP 2.63. The surface is smooth and uniform, due to the amorphous nature of the PVP. It has to be noticed that when the ratio of $FeAc_2$/PVP decreases from 2.63 to 0.43, the average diameter decreases as well. The average diameters are 440, 395, 260, 220 nm for the sample A1, A2, A3, A4 respectively.

Those samples prepared using a $FeAc_2$/PVP wt ratio of 2.63, 1.75, 0.83 and 0.43 have been then annealed under air flow up to 550°C (Samples B in table 1). It can be seen on the Figure 1b that all the nanofibers exhibit shrinkage and roughness but the nanofibers morphology observed before the annealing treatment remained unchanged. Compared to as-electrospun nanofibers (Fig.1a), the average diameter of each sample was reduced significantly due to the decomposition of the PVP component. Those average diameters are 240, 160, 115, 95 nm for the sample B1, B2, B3, B4 respectively. The average diameter decreases with a decrease of the amount of $FeAc_2$. These results indicate that the morphology of as-electrospun nanofibers is largely influenced by the solution concentration. In fact, the solution viscosity and surface tension change with the change of $FeAc_2$ content.

The crude samples A have been also pyrolysed under a 5% H_2+95% Ar atmosphere. The resulting samples are noted C in table 1. It has been previously reported that the direct reduction of iron trinitrate in a hydrogen atmosphere at 550°C for 5 h which results into the formation of pure iron nanofibers [16]. We report here for the first time the reduction of $FeAc_2$ in a tubular oven at 350°C for 4 h in a 5% H_2+95% Ar atmosphere. The black product, exhibiting a magnetic behavior in contact with a magnet, was observed by SEM (Fig.1c). Although a curved shape is observed, the fiber morphology is maintained during the reduction and the degradation of the polymer matrix. On the contrary to the SEM results observed in the case of the hematite nanotubes, the average diameter remains constant when the amount of $FeAc_2$ is reduced. We have measured 410, 430 and 320 nm for the sample C1, C2, C3 respectively.

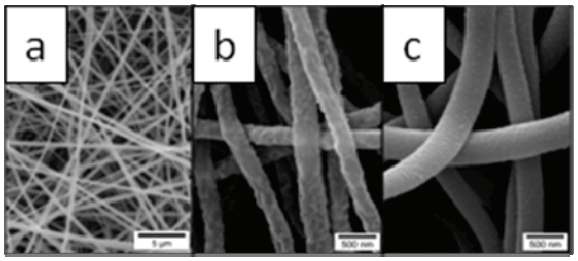

Figure 1. SEM images of the iron-based nanofibers, (a) before annealing treatment, (b) annealed under air atmosphere and (c) after treatment in an Ar/H_2 atmosphere.

The structure of the samples B1 to B4 was further investigated by XRD. XRD patterns shown in Figure 2a present the hematite structure of the nanofibers. All the peaks can be indexed to the phase-pure spinel α-Fe_2O_3 (JCPDS n°00-024-0072). The sharp peaks confirm the high crystallinity of the products. Comparing the patterns for the different $FeAc_2$ contents, one can deduce that varying the ratio has no influence on the crystalline structure of the nanotubes. To further identify the structure of the prepared nanofibers, a Raman spectroscopy study has been performed (Fig.2b). Most of phonon lines corresponding to the Hematite phase that belongs to the D^6_{3d} crystal space group are observed in the Raman spectrum, namely two A_{1g} modes (215 and 495 cm^{-1}) and three E_g modes (281, 394 and 596 cm^{-1}). Hematite is an antiferromagnetic material and the collective spin movement can be excited in so called magnon. As a result, the intense peak observed at 1320 cm^{-1} is related to a two-magnon scattering which arises from the interaction of two magnons created on antiparallel close spin sites [23a, b]. Compared to literature, the band positions shift slightly to lower wavenumbers probably due to the local heating resulting from the laser power (8mW) [20].

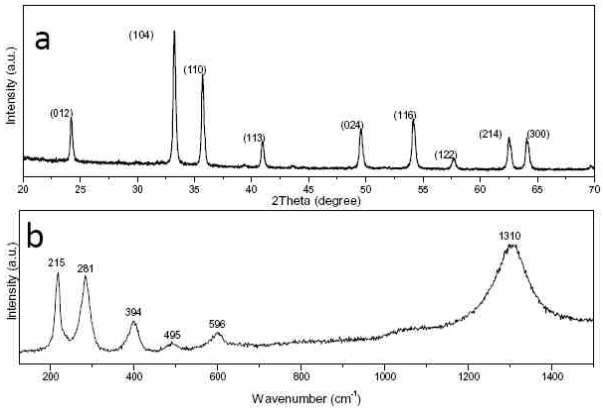

Figure 2. (a) XRD pattern and (b) Raman spectra of α-Fe_2O_3 nanotubes prepared with ratios ($FeAc_2$/PVP) = 2.63.

A conventional TEM study has been conducted to investigate more carefully the structure of those nanofibers. Figure 3a exhibits TEM images of α-Fe_2O_3 nanofibers that present hollow structure-like nanotubes. It has to be noticed that those tubular structures have a wall thickness which increases with the $FeAc_2$/PVP wt ratios. In fact, Figure 3a shows an increase of the wall dimension from 13 nm to 70 nm with the contents of $FeAc_2$ increased. This result presents a promising route for the production of hematite nanotubes with distinctive inner and outer surfaces.

A High Resolution TEM (HRTEM) study has been performed on those samples to investigate in details their structure. For example, the Figure 3b exhibits two specific orientations of α-Fe_2O_3 nanotubes synthesized with $FeAc_2$/PVP = 0.43. The nanofiber seems to be well-crystallized all along the principal axis and the following crystallographic planes have been indexed (a) d_{012}=3.68 Å, (b) d_{104}=2.70 Å and d_{110}=2.52 Å according to the JCPDS reference code n°00-024-0072 (Fig. 3b).

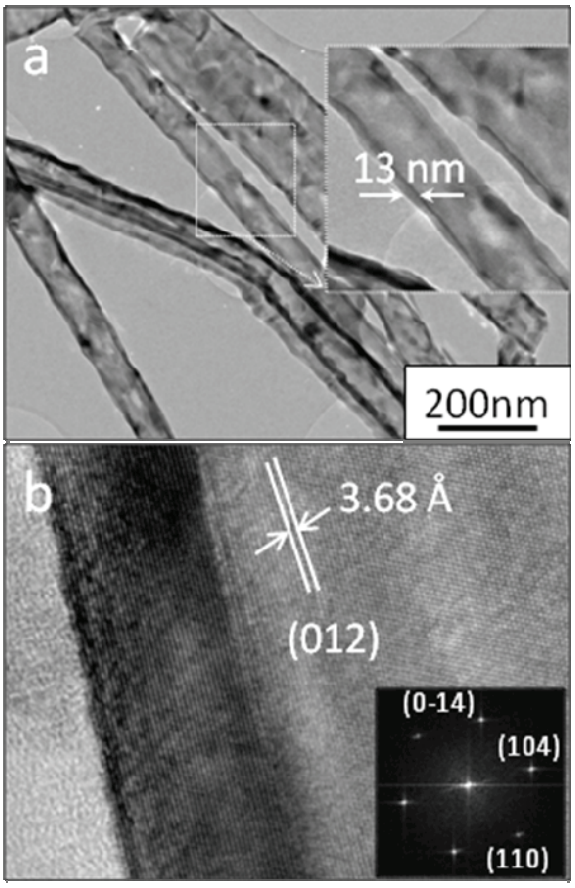

Figure 3. (a) TEM images of α-Fe_2O_3 hollow fibers prepared with wt ratios ($FeAc_2$/PVP) 0.43.and (b) corresponding HRTEM images.

Concerning the samples A that have been annealed under a 5% H_2+95% Ar atmosphere, TEM (Insert Fig.4) and Raman spectroscopy studies have been performed. Those samples finally contain small crystals of Fe_3C embedded in a carbon graphitic matrix when the nanofiber has been prepared with a ratio $FeAc_2$/PVP = 0.87. The

crystalline planes (002) and (200) of the Fe_3C orthorhombic phase (space group Pnma E, JCPDS n°00-003-0411) are shown. Moreover, these Fe_3C domains are surrounded with well-known concentric graphitic planes. As a consequence, the reduction in a hydrogen atmosphere of the as-electrospun PVP/ $FeAc_2$ is then responsible of the formation of polycrystalline Fe_3C nanofibers composed of carbon graphitic planes ensuring the Fe_3C nanoparticles stability and the nanofibers cohesion.

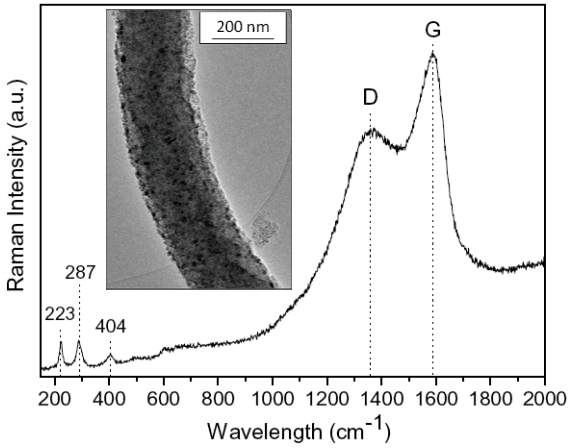

Figure 4. TEM images of α-Fe_2O_3 hollow fibers prepared with wt ratios ($FeAc_2$/PVP) 0.43.and (b) corresponding Raman spectrum.

On the same sample presented above, a Raman (Fig.) study has been conducted to confirm the observations made by TEM. Based on a previous study [24] peaks located at low wave numbers can be attributed to Fe_3C nanoparticles. The two bands marked D and G centered respectively at 1360 and 1594cm^{-1} confirm the presence of graphitic carbon in the nanofibers. The relative intensity of those two bands indicates that the structural disorder (D) of the crystallographic planes is less important than the strain (G) in the nanofibers.

4 CONCLUSIONS

We have successfully prepared iron based 1D nanostructures by electrospinning technique, varying the pyrolysis atmosphere. We have obtained tunable hematite nanotubes and polycrystalline Fe_3C nanofibers by a simple air or mixed (H_2/Ar) annealing treatments respectively. In the first case, the direct influence of the starting polymer solution on the tubular morphology is of main importance and allows varying the wall thickness. In the second case, for the first time, we achieve to obtain polycrystalline Fe_3C nanofibers composed of carbon graphitic planes ensuring the Fe_3C nanoparticles stability and the nanofibers cohesion. These results provide a promising lead for the future synthesis of a variety of Fe based nanofibers' morphology with controllable diameter and crystalline structure.

REFERENCES

[1] Xia, Y. N.; Yang, P. D. Adv. Mater. 2003, 15, 351.
[2] Wu, H.; Zhang, R.; Liu, X.; Lin, D.; Pan, W. Chem. Mater. 19, 3506, 2007,
[3] Li, D.; Herricks, T.; Xia, Y. Applied Physics Letters, 83, 4586, 2003/
[4] Henry, Y.; Ounadjela, K.; Piraux, L.; Dubois, S.;George, J. M.; Duvail, J. L. Eur. Phys. J. B 2001, 20, 35.
[5] Reich, D.H.; Tanase, M.; Hultgren, A.; Bauer, L.A.; Chen, C.S.; Meyer, G.J. J. Appl. Phys., 93, 7275, 2003.
[6] Xie, J.; Chen, C.; Varadan, V.K.; Yancey, J.; Srivatsan, M. Nanotechnology, 19, 105101, 2008.
[7] Brown, A.S.C.; Hargreaves, J.S.J.; Rijniersce, B. Catalysis Letters, 53, 7, 1998.
[8] Zheng, W.; Li, Z.; Zhang, H.; Wang, W.; Wang, Y.; Wang, C. Materials Research Bulletin, 44, 1432, 2009.
[9] Zboril, R.; Mashlan, M.; Petridis, D. Chem. Mater., 14, 969, 2002.
[10] Lin, C.R.; Tsai, T.C.; Chung, M.; Lu, S.Z. J. Appl. Phys, 105, 07B509, 2009.
[11] Jia, C.J. ; Sun, L.D.; Yan, Z.G.; You, L.P.; Luo, F.; Han, X.D.; Pang, Y.C.; Zhang, Z.; Yan, C.H. Angew. Chem. Int. Ed, 44, 4328, 2005.
[12] Sui, Y.C.; Skomski, R.; Sorge, S.D.; Sellmyer, D.J. J. Appl. Phys., 95, 7151, 2004.
[13] Suber, L.; Imperatori, P.; Ausanio, G.; Fabbri, F.; Hofmeister, H. J. Phys. Chem. B, 109, 7103, 2005.
[14] Jia, C.J. ; Sun, L.D.; Yan, Z.G.; Pang, Y.C.; You, L.P.; Yan, C.H. J.Phys. Chem. C, 111, 13022, 2007.
[15] Fan, H.M.; You, G.J.; Li, Y.; Zheng, Z.; Tan, H.R.; Shen, Z.X.; Tang, S.H.; Feng Y.P. J.Phys. Chem. C, 113, 9928, 2009.
[16] Liu, L.; Kou, H.Z.; Mo, W.; Liu, H.; Wang, Y. J. Phys. Chem. B, 110, 15218, 2006.
[17] Graeser, M.; Bognitzki, M.; Massa, W.; Pietzonka, C.; Greiner, A. Adv. Mater., 19, 4244, 2007.
[18] Tang, B.; Wang, G.; Zhuo, L.; Ge, J.; Cui, L. Inorg. Chem, 45, 5196, 2006.
[19] Y. Qiu, J. Yu, C. Tan, X. Zhou, X. Bai, E. Wang, Nanotechnology, , 20, 345603, 2009
[20] Wang, Z.; Liu, X.; Lv, M.; Chai, P.; Liu, Y.; Zhou, X.; Meng, J. J. Phys. Chem. C, 112, 15171, 2008.
[21] Kowalewski, T.A.; Blonski, S.; Barral, S. Bull. Pol. Ac.: Tech, 53, 385, 2005.
[22] Santala, E.; Kemell, M.; Leskela, M.; Ritala, M. Nanotechnology, 20, 035602, 2009.
[23] S. Cavaliere-Jaricot, A. Brioude, P. Miele, Langmuir, , 25, 5, 2551-2553, 2009.
[24] Doeff, M. M.; Wilcox, J. D.; Yu, R.; Aumentado, A. ; Marcinek, M. ; Kostecki, M. J Solid State Electrochem., 12, 995–1001, 2008.